Deep traps and persistent photocapacitance in β-$(Al_{0.14} Ga_{0.86})_2O_3/Ga_2O_3$ heterojunctions

A. Y. Polyakov, N. B. Smirnov, I. V. Schemerov, A. V. Chernykh [iD], E. B. Yakimov [iD], A. I. Kochkova,
Jiancheng Yang, Chaker Fares [iD], F. Ren [iD], and S. J. Pearton [iD]

View Online   Export Citation   CrossMark

Deep traps and persistent photocapacitance in β-(Al$_{0.14}$ Ga$_{0.86}$)$_2$O$_3$/Ga$_2$O$_3$ heterojunctions

View Online   Export Citation   CrossMark

A. Y. Polyakov,[1] N. B. Smirnov,[1] I. V. Schemerov,[1] A. V. Chernykh,[1,2] (ID) E. B. Yakimov,[1,3] (ID) A. I. Kochkova,[1]
Jiancheng Yang,[4] Chaker Fares,[4] (ID) F. Ren,[4] (ID) and S. J. Pearton[4,a)] (ID)

AFFILIATIONS

[1]National University of Science and Technology MISiS, 4 Leninskiy Ave., Moscow 119049, Russia
[2]Pulsar Scientific and Production Enterprise, Joint Stock Company, Okruzhnoy Way, House 27, Moscow 105187, Russia
[3]Institute of Microelectronics Technology and High Purity Materials, Russian Academy of Science, 6 Academician Ossipyan str.,
Chernogolovka, Moscow Region 142432, Russia
[4]Department of Materials Science and Engineering, University of Florida, Gainesville, Florida 32611, USA

[a)]Author to whom correspondence should be addressed: spear@mse.ufl.edu

ABSTRACT

Persistent photocapacitance (PPC) was observed in β-(Al$_{0.14}$Ga$_{0.84}$)$_2$O$_3$/n$^+$Ga$_2$O$_3$ heterojunctions at low temperatures. The effect is seen in capacitance-frequency measurements under illumination and in admittance spectra after illumination. In the latter case, the capacitance versus frequency curve after illumination returned to its dark values only at temperatures between 225 and 275 K. Prominent hole-trap-like peaks in optical deep level transient spectroscopy (ODLTS) near 130 K were attributed to quenching with temperature of the PPC effect. The phenomena were assigned to electrons being excited from deep traps in the (Al$_{0.14}$Ga$_{0.86}$)$_2$O$_3$ barrier into the two-dimensional electron gas (2DEG) in the Ga$_2$O$_3$ substrate. The reverse process then involves excitation of non-equilibrium electrons in the 2DEG back into the ternary barrier layer and subsequent re-capture by the host deep traps. The effective barrier height for this recovery process was ∼0.2 eV, as estimated from ODLTS measurements. The spectral dependence of the effect suggests the presence of deep traps with optical ionization thresholds near 1 eV and ∼2.3 eV. The shift of the threshold voltage necessary to deplete the 2DEG as a function of the photon energy during illumination at room temperature indicates that the most prominent centers in the barrier have an optical ionization energy near 2.3 eV and a sheet density of ∼10^{12} cm^{-2}. In microcathodoluminescence (MCL) spectra of the heterojunction, a blue shift by 0.2 eV of the MCL band near 3.1 eV dominant in the substrate and the emergence of a weak MCL peak near 4.8 eV were observed. Electron beam induced current measurements point to the presence of small local areas where the 2DEG formation is handicapped due to Al composition variations or to defects.

Published under license by AIP Publishing. https://doi.org/10.1063/1.5080941

I. INTRODUCTION

Monoclinic β-Ga$_2$O$_3$ has been intensely studied in recent years due to the favorable properties for high-power transistors and solar-blind photodetectors.[1–5] Of particular interest are heterojunctions of β-Ga$_2$O$_3$ with β-(Al$_x$Ga$_{1-x}$)$_2$O$_3$ in a wide range of Al compositions for the bandgap range of 4.6-4.8 eV for x = 0 to 5.5 eV for x = 0.54 (the range of compositions where the β-polytype has been shown to be dominant).[6,7] These compounds form with β-Ga$_2$O$_3$ type I hetrojunctions with reasonably high conduction band offsets,[7] which makes it possible to fabricate high electron mobility transistors (HEMTs) with two-dimensional electron gas (2DEG) at the heterointerface formed by modulation n-type doping.[7–13]

This doping can either be from Si donors in (Al$_x$Ga$_{1-x}$)$_2$O$_3$ near the heterointerface with Ga$_2$O$_3$[13] or intentional, usually achieved by doping of the β-(Al$_x$Ga$_{1-x}$)$_2$O$_3$ thin barrier.[7–12] The existence of 2DEG at the interface of these heterojunctions has been demonstrated by the observation of Shubnikov-de Haas oscillations,[9,10] with good low temperature 2DEG mobility,[9,10] and promising performance of HEMTs on semi-insulating Ga$_2$O$_3$ buffers doped with Fe.[8–12] The physical properties of (Al$_x$Ga$_{1-x}$)$_2$O$_3$/Ga$_2$O$_3$ heterojunctions are therefore of great interest.

In this paper, we present capacitance-voltage and admittance spectra measurements on (Al$_{0.14}$Ga$_{0.86}$)$_2$O$_3$/Ga$_2$O$_3$ structures at different temperatures in the dark and under illumination. The observed persistent photocapacitance (PPC) is attributed to the

excitation of electrons from deep traps in the $(Al_{0.14}Ga_{0.86})_2O_3$ barrier into the Ga_2O_3. We also report microcathodoluminescence (MCL) spectra and diffusion length of nonequilibrium carriers by electron beam induced current (EBIC). The former shows the presence of a weak near-band edge luminescence peak due to $(Al_{0.14}Ga_{0.86})_2O_3$, while the latter points to a reasonably long diffusion length in the ternary barrier.

II. EXPERIMENTAL

The samples were obtained from Novel Crystal Technology, Inc. (Japan). The 0.055-μm-thick $(Al_{0.14}Ga_{0.86})_2O_3$ barrier was grown by molecular beam epitaxy (MBE) on (010)-oriented Sn doped (donor concentration 6.3×10^{18} cm^{-3}) β-Ga_2O_3 substrates prepared by edge-defined film-fed growth (EFG). The Si donor concentration in the ternary $(Al_{0.14} Ga_{0.86})_2O_3$ MBE film was 10^{17} cm^{-3}. The back Ohmic contact was prepared by e-beam evaporation of Ti/Au (20 nm/50 nm) on Ar plasma treated and 450 °C annealed substrate back surfaces. Two types of diodes were prepared. Smaller diameter (100 μm) Ni/Au(80/420 nm) Schottkies overlapped onto field plates (SiO$_2$ 40 nm, SiN$_X$ 360 nm) were used for device breakdown and reverse recovery measurements. For material characterization measurements, circular semitransparent Ni Schottky contacts (1.2 mm diameter, 30 nm thickness) were fabricated on the front $(Al_{0.14}Ga_{0.86})_2O_3$ side by e-beam evaporation using a shadow mask.[14] We label the ternary barrier layers as the AlGaO barrier and the heterojunction (HJ) as AlGaO/GaO.

The samples were characterized by capacitance-frequency (C-f) and capacitance-voltage (C-V) over the frequency range of 20 Hz-1 MHz, by admittance-spectra (AS)[15] measurements, deep level transient spectroscopy with electrical (DLTS) and optical (ODLTS) injection,[16] and current-voltage (I-V) measurements. C-V, C-f, AS, and I-V measurements were performed in the dark, under illumination with intense monochromatic light with photon energies in the 1.35-3.4 eV, and after such illumination. DLTS and ODLTS measurements were performed at 10 kHz to reduce the effects of series resistance.[16] Optical excitation in ODLTS was done by high-power light emitting diode (LED) with a peak photon energy of 3.4 eV or by UV LED with a peak photon energy of 4.8 eV. The spectral dependences of C-f, C-V, and I-V measurements were obtained using a set of high-power (optical power 250 mW) LEDs and were normalized by the number of photons for each LED photon energy. MCL spectra were measured at 25 °C at probing beam accelerating voltages in the range of 0.7 kV to 10 kV and were compared to MCL spectra taken on Ga_2O_3 substrate without the $(Al_{0.14}Ga_{0.86})_2O_3$ barrier. Diffusion length values were measured by EBIC signal linear scanning along the surface away from the Schottky diode edge.[17–19]

III. RESULTS AND DISCUSSION

A. I-V characteristics

For the device measurements, Fig. 1 shows the temperature dependence of both forward and reverse current density. The barrier height assuming thermionic emission was 1.24 eV, with an ideality factor of 1.3, Richardson's constant of 48.56 A cm^{-2} K^{-2}, and a zero-bias barrier height, $q\phi_{bo}$, of 1.15 eV. The reverse
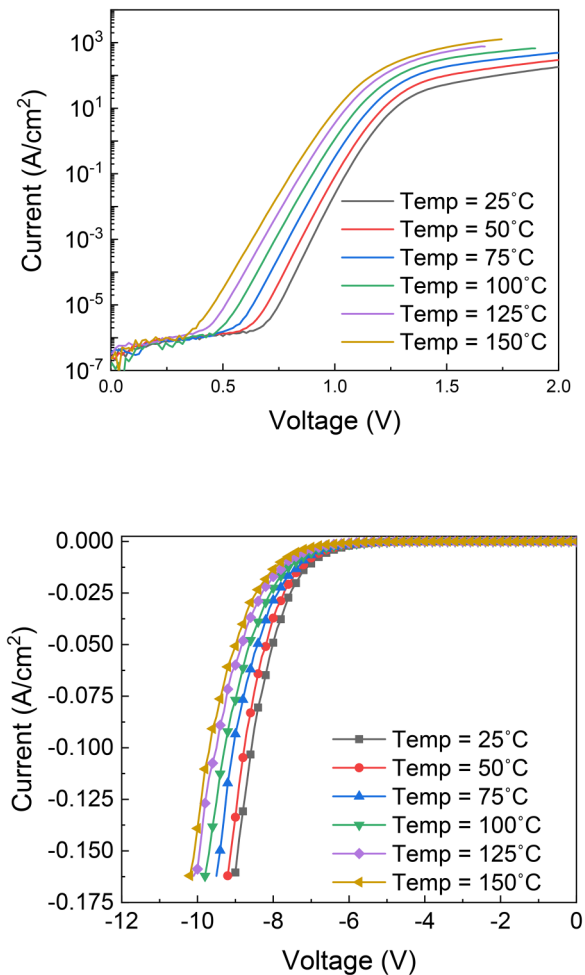

FIG. 1. Temperature dependence of forward (top) and reverse (bottom) leakage current density in vertical heterostructure diodes.

breakdown showed a positive temperature coefficient of 0.072 V/°C. The reverse recovery waveform, Fig. 2, corresponded to a reverse recovery lifetime of 22 ns for the diode. This value contains a component from the minority carrier lifetime for Ga_2O_3, which is reported to be in the range of 30-215 ps.[20–22] The larger Schottky diode reverse current density at −1 V and room temperature was 10^{-10} A/cm^2 but increased to 10^{-5} A/cm^2 at −4 V, with reverse current at voltages exceeding −1 V increasing exponentially with voltage, indicating the presence of tunneling. The Schottky barrier height determined from the spectral dependence of the square root of the photocurrent yield versus photon energy (the Fowler plot[23]) was ~1.45 eV. The photocurrent increased steeply for photon energies around 2.3 eV. The ideality factor in forward I-Vs was 1.2. The temperature dependence of the saturation current in forward I-Vs was 0.8 eV, lower than determined from the Fowler plot and indicating either non-uniform barrier height across the heterojunction area[8] or the forward current flow via tunneling with thermal
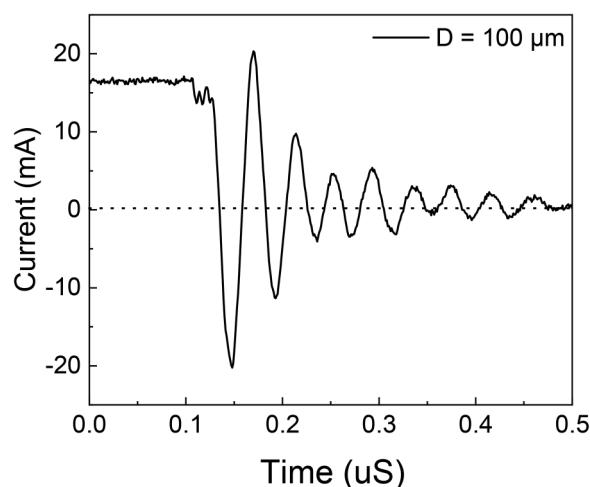
FIG. 2. Reverse recovery of heterostructure diodes switched from −10 V to +1 V. The extracted reverse recovery lifetime is ∼22 ns.

excitation to the level near E_c-0.8 eV. The difference in I-V performance of the passivated low-area diodes and unpassivated large-area diodes can be attributed to the different impact of local Al composition fluctuations (see below) or to the slight difference in the Schottky diodes fabrication procedure.

B. C-f, C-V, admittance spectra measurements: 2DEG and PPC

Capacitance-frequency measurements revealed the presence of two prominent capacitance steps whose positions depended on temperature. Figure 3(a) shows C-f curves measured at 85 K in the dark and under illumination. Figures 4(a) and 4(b) show admittance spectra. Standard admittance spectra analysis[15] yielded an activation energy $E_a = 0.04$ eV and electron capture cross section $\sigma_n = 1.2 \times 10^{-19}$ cm^2, for the low frequency step in capacitance/peak in admittance [Figs. 4(a) and 4(b)]. This activation energy is reasonably close to the activation energy of Sn donors in β-Ga$_2$O$_3$.[24] For the second step, the activation energy was $E_a = 0.15$ eV with $\sigma_n = 3.2 \times 10^{-18}$ cm^2. It is likely that this step/peak is associated with electron transport over the AlGaO/GaO heterointerface and over the AlGaO layer adjacent to the interface. The 25 °C concentration profile calculated from C-V measurements is shown in Fig. 5(a). The AlGaO barrier layer is almost totally depleted even at low forward voltages. The charge concentration deep inside the Ga$_2$O$_3$ is close to the target doping, 6.3×10^{18} cm^{-3}. The charge concentration in the interface region peaks at 2×10^{19} cm^{-3} and shows the charge concentration in the 2DEG region most likely formed due to Si donors build-up at the HJ AlGaO/GaO interface on the AlGaO layer side producing modulation doping in the Ga$_2$O$_3$ substrate.[13] Thus, at low reverse biases, the space charge region (SCR) boundary is located near the AlGaO/GaO interface and the high frequency 0.15 eV peak in admittance spectra in Fig. 4(b) comes from the interface states or states in the AlGaO
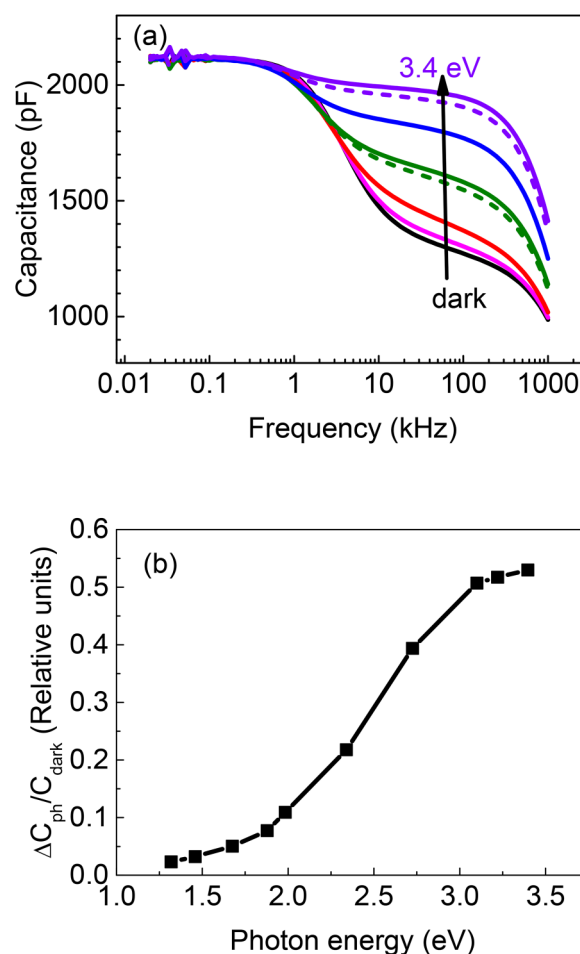

FIG. 3. (a) 85 K C-f curves measured at −0.2 V in the dark (black line), under illumination with 1.35 eV LED (magenta line), under illumination with 1.88 eV LED (red line), under illumination with 2.3 eV LED (olive line) and 20 min after (dashed olive line), under illumination with 2.7 eV LED (blue line), under illumination with 3.4 eV LED (violet line) and 20 min after 3.4 eV LED illumination (dashed violet line); (b) excitation spectra of normalized photocapacitance signal.

layer near the interface becoming too slow to be able to follow the probing electric field frequency in admittance measurements.[15] Integrating the profile in the 2DEG region gives sheet 2DEG concentration of 2×10^{12} cm^{-2}, close to that reported in Ref. 13 and lower than that observed in HEMT structures with δ-doped barriers.[8–12] Due to the high parallel conductance of the heavily n-type doped Ga$_2$O$_3$ substrate, it was not possible to extract 2DEG concentration and mobility from Van der Pauw measurements, as done for structures on semi-insulating substrates.[8–13]

Figure 5(b) shows the concentration profile as a function of applied bias in the dark and under monochromatic illumination with two different photon energies. If one determines the threshold voltage V_{th} for the depletion of the 2DEG as the point where the concentration becomes equal to the concentration in the substrate,
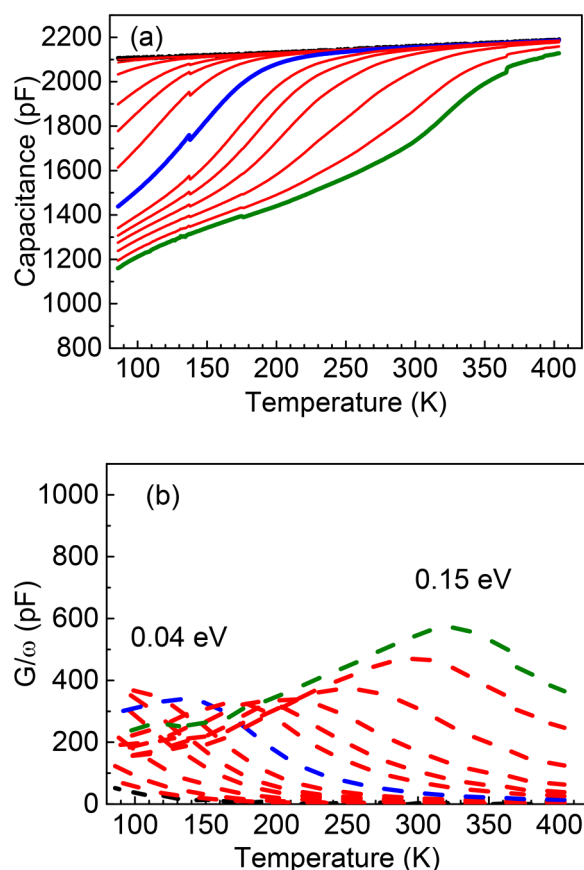
FIG. 4. (a) Capacitance at −0.2 V dependence on temperature for frequencies f = 0.2 kHz (the uppermost line, black line), 0.3 kHz, 0.5 kHz, 1 kHz, 2 kHz, 3 kHz, 5 kHz, 10 kHz (blue line), 30 kHz, 50 kHz, 100 kHz, 200 kHz, 300 kHz (the lowermost line, olive line); (b) AC conductance G divided by the angular frequency for the same set of frequencies (0.2 kHz is the leftmost line, black line, 300 kHz is the rightmost line, olive line, the data for 10 kHz are shown as blue line).

FIG. 5. (a) Room temperature concentration profile (the plateau corresponds to the substrate region, the accumulation region corresponds to 2DEG); (b) concentration dependence on applied voltage measured in the dark (black line), under 2.3 eV LED illumination (olive line), under 3.4 eV illumination (violet line); (c) spectral changes of the absolute value of the threshold voltage shift ΔV_{th} with illumination (under illumination the threshold voltage shifts to more negative values); measurements at 10 kHz.

this V_{th} in the dark is −4 V. Illumination shifts the threshold voltage to more negative values because of the charge build-up on deep traps in the barrier.[25] Changes in the threshold voltage start at a photon energy of 2.3 eV and saturate at the absolute value of $\Delta V_{th} = 0.76$ V for photon energies exceeding 3.1 eV [Fig. 5(c)]. This threshold voltage shift can be converted into the charge build-up on deep traps[25] and then recalculated into the sheet trap density—this was $\sim 10^{12}$ cm^{-2}.

The structures showed photocapacitance at all temperatures. For 85 K, the amount of the effect is illustrated in Fig. 3(a) showing C-f characteristics in the dark, under illumination with high-power LEDs for a short time (10 s) and after 20 min wait in the dark after illumination. The signal in photocapacitance appeared starting from a photon energy of 1.35 eV, the onset of strong photocapacitance corresponded to photon energies > 2 eV, while the signal saturated at 3.4 eV. The capacitance changes occurred only for the
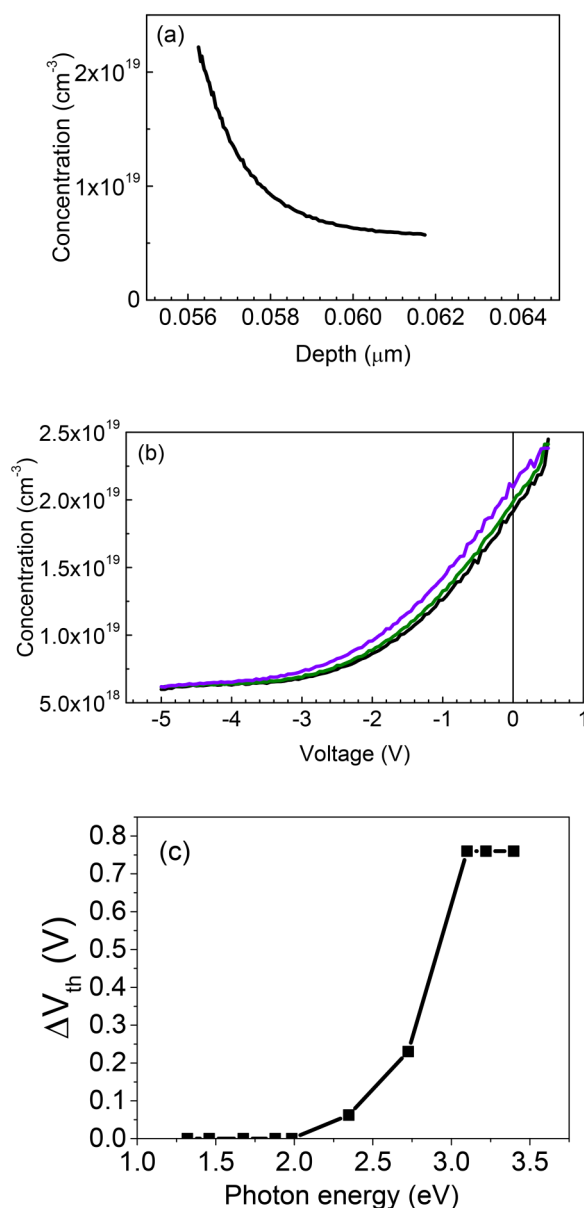
high-frequency step in C-f dependence, i.e., for states adjacent to the heterointerface. Photocapacitance induced by illumination for this step was persistent and did not decrease at 85 K for a long time [Fig. 3(a) shows the persistent photocapacitance (PPC) measured
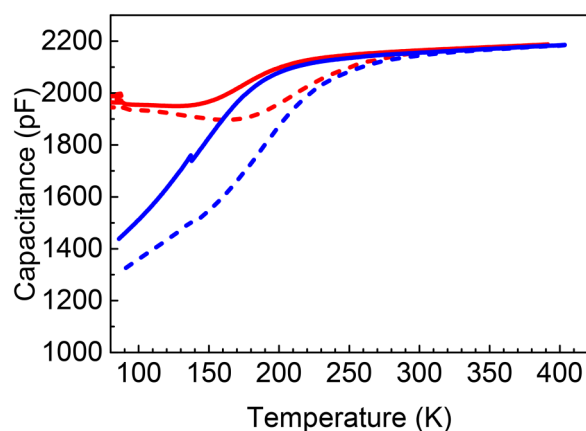
FIG. 6. Dark (dashed curves) and PPC (solid lines) capacitance versus T dependences for measurement frequencies of 10 kHz (red lines) and 30 kHz (blue lines).
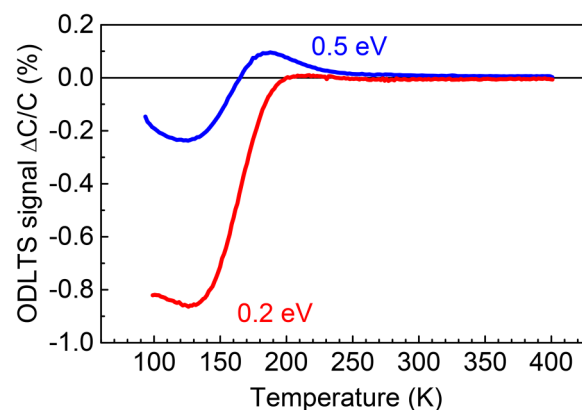

FIG. 7. ODLTS spectra measured at −0.2 V, with time windows 3 s/30 s, for excitation with 3.4 eV LED (red line) and 4.8 eV (blue line) showing hole-trap-like signal corresponding to an activation energy of 0.2 eV (negative peak according to our convention in this paper) and electron trap signal (positive peak) corresponding to an activation energy of 0.5 eV.

after 20 min wait as dashed curves]. It was interesting, of course, to determine the spectral dependence of the effect. This is illustrated in Fig. 3(b) showing the photocapacitance C_{ph} normalized to the dark capacitance C_{dark} as a function of photon energy. It can be seen that the PPC capacitance starts to measurably increase for photon energies above ~1.5 eV and strongly picks up for photon energies above 2.3 eV, which allows to get some idea of the levels of states participating in the phenomenon.

One would expect that the decay time of persistent photocapacitance should become faster as the temperature increases. Once this decay time becomes comparable to the probing frequency in capacitance measurements the capacitance measured after illumination should become close to the dark capacitance. Qualitatively the temperature dependence of the effect is given by comparison of admittance spectra measured upon cooling down in the dark and the spectra measured after illumination with the 3.4 eV LED at 85 K. These are shown in Fig. 6 for probe frequencies of 10 kHz and 30 kHz. The PPC capacitance curves merge with the dark capacitance curves at temperatures between 225 and 275 K, with the merging temperature increasing with frequency as expected.

C. ODLTS and DLTS

The activation energy involved in this PPC temperature quenching process can be obtained from ODLTS spectra measurements carried out with photoexcitation produced by high-power 3.4 eV LED and 4.8 eV UV LED, as depicted in Fig. 7. The spectra were taken with a steady-state bias of −0.2 V placing the SCR boundary near the interface in the HJ AlGaO/GaO judging by the C-V data in Fig. 5. Both types of excitations produce a prominent hole-trap-like peak (capacitance decreases with time after illumination pulse,[16] a negative peak according to the convention in the figure) in ODLTS corresponding to an activation energy of 0.18-0.2 eV. Hole-trap-like peaks with similar activation energy were reported in Hydride Vapor Phase Epitaxy (HVPE) β-Ga$_2$O$_3$ films.[19] Those were attributed to the transition of hole-related polarons into free

valence band holes. However, these peaks in Ga$_2$O$_3$ showed a doublet structure and were observed at lower temperatures. This most likely excludes polaronic states in the Ga$_2$O$_3$ substrate as the source of the peaks observed in the heterostructures.

X-ray photoelectron spectroscopy (XPS) measurements of the same heterostructures[26] showed that the bandgap of the ternary solution barrier is 5 eV, with the bandgap of the Ga$_2$O$_3$ substrate being 4.6 eV. The 3.4 eV LED photon energy is below the bandgap of both the substrate and the barrier and should not generate polarons in the valence band. The peaks in ODLTS spectra in Fig. 7 are similar for excitation with 3.4 and 4.8 eV photons (the difference in the magnitude of the peaks comes from the difference in the optical power, 250 mW for 3.4 eV, 8 mW for the 4.8 eV LED). We believe that these peaks come from the photocapacitance being persistent and only slowly returning to the dark value after the LED pulse. This persistent photocapacitance relaxation should have the same sign as for a hole trap related signal (the capacitance decreases with time after the pulse) and will look like a negative peak in the spectra. Then, the measured activation energy should be close to the barrier height for the slow recombination of persistent electrons. The mechanism of persistent photoconductivity may be similar to that observed previously for AlGaN/GaN heterojunctions,[25,27] namely, electrons in the ternary barrier are excited from deep traps in the barrier and transferred to the 2DEG region, but cannot return to the barrier and be recaptured by their host states unless they overcome the barrier close to the conduction band discontinuity ΔE$_c$ minus the Fermi level in 2DEG. In that case, ΔE$_c$ in our heterojunction should be ~0.18 eV plus the depth of the highest filled energy level in the triangular quantum well with 2DEG near the interface. According to several estimates,[7] the conduction band offset for the barrier composition used here should be between 0.3 and 0.4 eV and these values can be easily reconciled with the activation energy observed in ODLTS. The origin of the capacitance/admittance step/peak activation energy of 0.15 eV in

dark admittance spectra in Figs. 4(a) and 4(b) could be also related to the overcoming of this effective conduction band offset.

An additional feature observed for UV excitation in the low temperature ODLTS spectra is an electron-trap-like peak near 180 K, corresponding to electron traps with the level E_c-0.5 eV and electron capture cross section of 2.5×10^{-14} cm^2. This center is likely located in the barrier.

The structure was not well suited for deep traps analysis because a strong freeze-out of capacitance occurred below 200-250 K, which presents an obstacle even when DLTS spectra were measured at 10 kHz (blue curve in admittance spectra in Fig. 4), the lowest frequency at which the dark DLTS spectra could be measured with reasonable sensitivity of $N_t/N_d \sim 5 \times 10^{-4}$ in our DLTS setup[16] (N_t is density of deep traps, N_d is the density of shallow donors determining the width of the space charge region). The barrier layer was almost fully depleted even at zero volts bias and could be probed only with high forward bias pulses, while the concentration of donors in the substrate was high, decreasing the sensitivity. Figure 8 compares DLTS spectra taken with bias of −4 V and pulsing of the voltage to −1 V (the SCR boundary for both the steady-state bias and pulse bias being within the Ga$_2$O$_3$ substrate according to the data of Fig. 5) and the spectrum obtained for steady-state reverse bias of −2 V (near the AlGaO/GaO interface from C-V profiling experiments summarized in Fig. 5) and pulsing to +2 V into the AlGaO barrier. The first regime probes the deep states in the substrate, and the second also probes the deep electron traps in the barrier. Both spectra show two peaks corresponding to electron traps with levels E_c-0.74 eV ($\sigma_n = 4 \times 10^{-15}$ cm^2) and E_c-0.95 eV [$\sigma_n = (2\text{-}4) \times 10^{-16}$ cm^2] whose signatures are similar to the signatures of E2 and E3 traps in n-Ga$_2$O$_3$[18–24] and thus should belong to electron traps in the substrate. The E2 trap signal is more pronounced in the spectra taken with high forward voltage pulse more likely to recharge the states closer to the interface with the barrier layer. The high peak in these DLTS spectra observed at
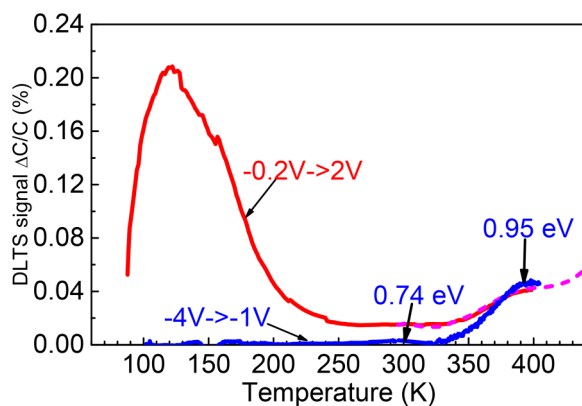
∼150 K for measurements with a high forward bias pulse of + 2 V (Fig. 8) is distorted by the strong capacitance freeze-out in this range, and the parameters of this trap in the barrier could not be reliably determined.

Some additional information about the deep traps spectra in the barrier can be gleaned from the C-f spectra in Fig. 3, from the shift of the threshold voltage in C-V characteristics [Fig. 5(b)], and from reverse photocurrent spectra. All these measurements show a prominent optical threshold near 2.3 eV. The sheet concentration of such traps estimated from the threshold voltage shift under illumination is ∼10^{12} cm^{-2}.

D. MCL spectra and images; EBIC images and profiles

MCL spectrum measured with a low probing beam voltage of 0.7 kV generating charge carriers predominantly in the barrier layer is compared to the spectrum obtained under the same conditions in the substrate in Fig. 9 (for the latter measurements, the back side of the substrate was used). In both spectra, the dominant feature was the peak near 3 eV. The peak position was blue shifted from 3.1 eV to 3.3 eV when switching from the substrate to the heterojunction. In addition, in the heterojunction MCL spectrum, a weak peak near 4.8 eV was detected and comes from near-band edge recombination in the barrier. When measuring MCL spectra in different places of the heterojunction, there were points where the 3 eV peak was close to the position of the peak in the substrate while the 4.8 eV peak could not be detected (Fig. 9). This suggests that locally the Al composition in some points in the barrier could be much lower and close to pure Ga$_2$O$_3$.

In EBIC measurements performed between the Schottky diode on the top and the back Ohmic contact, the beam induced current was very small and only appeared at reverse voltages > −0.5 V. The EBIC image taken at −0.8 V and beam accelerating voltage of 36 kV is shown in Fig. 10. There are groups of bright spots (places with higher induced current) with an average density of around 10^8 cm^{-2}. In a sample with a 2DEG at the barrier/substrate
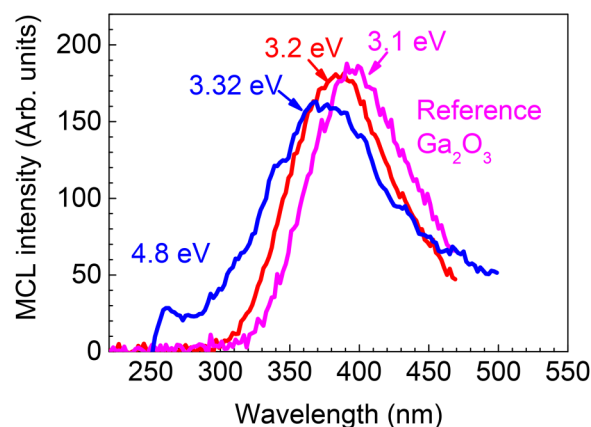

FIG. 8. DLTS spectra taken with bias −4 V and pulsing to −1 V (probing the Ga$_2$O$_3$ substrate, blue line) and −2 V with pulsing to + 2 V (probing the interface and the barrier layer, solid red line—measurements to 400 K, dashed magenta line—measurements in hot stage); the spectra were taken with time windows 1.75 ms/17.5 ms, an injection pulse length of 3 s, at a probing frequency of 10 kHz.

FIG. 9. Room temperature MCL spectra for reference Ga$_2$O$_3$ substrate (magenta line) and for the (Al$_{0.14}$Ga$_{0.86}$)$_2$O$_3$/Ga$_2$O$_3$ heterojunction measured in two places across the surface (red line and blue line).
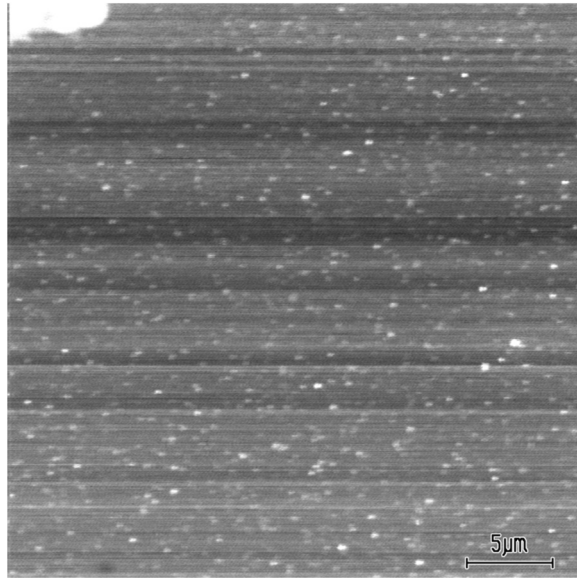
FIG. 10. EBIC image of the HJ AlGaO/GaO obtained with an accelerating SEM beam voltage of 36 kV and a probing beam current of 1 nA.

interface, the EBIC current transported by holes[17] will be extremely low in the vertical transport arrangement because of the efficient recombination of holes in the 2DEG. The existence of bright spots in the EBIC image in Fig. 10 suggests that there are places where the hole current can flow more easily, i.e., places where the 2DEG is not formed either because of the presence of defects or because of the Al composition in the barrier being lower. This correlates with inhomogeneity observed in the MCL spectra in Fig. 9. Under these observation conditions (Ohmic contact at the back surface of the sample), determining the diffusion length of nonequilibrium
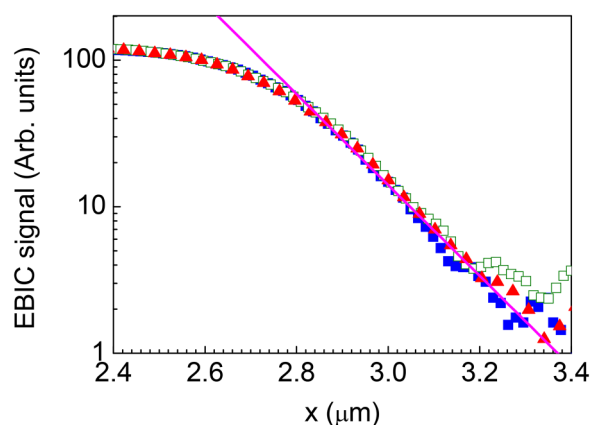

FIG. 11. EBIC current dependence on the distance to the edge of the Schottky diode (x) measured in several places (blue, red, and olive symbols), the diffusion length estimated from the slope (magenta line) is 140 nm.

charge carriers by measuring the dependence of EBIC collection efficiency on the probing beam accelerating voltage[17] is not practicable. To roughly estimate this parameter for the barrier layer, we measured the diffusion length from the decay of the EBIC signal when moving the probing SEM beam along the surface away from the edge of the Schottky barrier.[17] Figure 11 shows this measurement with a beam accelerating voltage of 6 kV (the results are presented for the SEM beam located in three different locations). The slope of the plot in semi-logarithmic scale yields a diffusion length of $L_d = 0.14\,\mu m$, a rough estimate considering the measurement conditions. This is lower than the diffusion lengths in high-quality thick Ga_2O_3 films grown by HVPE, typically, 0.4-6 μm.[17,18,28]

IV. SUMMARY AND CONCLUSIONS

In β-$(Al_{0.14}Ga_{0.86})_2O_3/Ga_2O_3$ heterojunctions with barriers grown by MBE on heavily n-type doped substrates, the barrier layer is depleted of electrons at 0 V applied bias on Ni Schottky diodes and a 2DEG region with a peak density near $2 \times 10^{19}\,cm^{-2}$ is formed at the interface, due to modulation doping caused by Si donors pile-up near the interface on the barrier side.[13] The threshold voltage corresponding to the depletion of the 2DEG region in the dark shifts to more negative voltages under illumination. Respective spectral dependence of the threshold voltage in Fig. 5(c) shows a prominent optical threshold near 2.3 eV corresponding to electrons being removed from deep traps in the barrier. This signal saturates near photon energy of 3 eV, with a sheet density of respective traps $\sim 10^{12}\,cm^{-2}$ corresponding to a bulk density of traps of $2 \times 10^{17}\,cm^{-3}$ if they are uniformly distributed in the barrier. Capacitance versus frequency steps corresponding to energies of 0.04 and 0.15 eV are likely related to the trapping/detrapping of electrons by the Sn donors in the substrate and to overcoming the potential barrier between the ternary and the substrate, respectively. These energies should be close to the conduction band offset minus the energy of the highest filled electron level in the 2DEG region.

At low temperatures, illumination causes persistent photocapacitance, with optical thresholds near 1.35 eV and 2.3 eV, due to electrons excited from deep traps in the ternary barrier layer and transported to the 2DEG. The return of the excited electrons to their host centers is prevented by the potential barrier between the ternary film and the 2DEG region. The spectra of the PPC excitation effect show several deep traps in the barrier with optical ionization energies between 1 eV and 3.1 eV, the strongest changes induced by photons with energy $\gtrsim 2.3$ eV. The PPC effect is quenched between 225 and 275 K. The dominant hole-trap-like peaks near 130 K in ODLTS spectra are attributed to this quenching of the PPC. The activation energy for these features is associated with the effective barrier height between the ternary layer and the 2DEG region (should be approximately equal to the conduction band offset and Fermi level position in 2DEG), which then should be close to 0.2 eV, similar to values obtained from XPS measurements performed on $(Al_xGa_{1-x})_2O_3/Ga_2O_3$ heterojunctions.[7]

These deep traps in the AlGaO barrier can produce an adverse effect on AC performance of AlGaO/GaO HEMTs causing switching delays in transistors operating at a high drain current and a high gate voltage because of possible electron capture by deep traps under the gate and deep traps in the transistor access region between the gate

and the drain, as is the case in GaN-based HEMTs.[29] The observed changes of the threshold voltage with illumination can cause additional instabilities in the AlGaO/GaO HEMTs operation. Our experiments do not provide information on deep traps spectra in semi-insulating Ga_2O_3 buffers doped with Fe that are used in real-life HEMTs, because our substrates were highly n-type conducting. However, for semi-insulating Ga_2O_3(Fe) substrates, a high potential role of the deep E2 electron traps in electron capture/emission in HEMTs has been discussed in Refs. 30–33. These E2 traps are related to Fe[30–32] and also are present in our conducting substrates.

MCL spectra show a blue shift of the dominant band near 3.1 eV in the substrate to 3.3 V in the heterojunction and the appearance of a weak UV peak near 4.8 eV related to the near-bandedge luminescence in the barrier. There were regions where the blue shift is much lower and the UV peak is not detected, indicating the presence of defects at the heterointerface decreasing the band bending and the formation of the 2DEG, such as places with lower local Al composition. Since the magnitude of the EBIC signal is determined by the efficiency of collectron by the top Schottky diode of the holes created by the SEM beam[17] and since this collection efficiency is handicapped by the presence of the 2DEG region where the holes recombine very efficiently, the character of the EBIC image suggests the presence of small local regions where the 2DEG formation is suppressed. This is a concern for Ga_2O_3 HEMTs because the current flow in the transistor channel will proceed via percolation, characterized by low effective 2DEG mobility.

The ternary barrier of the heterojunctions contains deep traps located between $\sim E_c$-1 eV and E_c-3.1 eV. These enhance the recombination of nonequilibrium charge carriers, leading to a lower diffusion length in the $(Al_{0.14}Ga_{0.86})_2O_3$ film compared to high quality Ga_2O_3 films (0.14 μm versus 0.4-0.6 μm). Additional optimization of the ternary barrier growth to suppress the 2DEG inhomogeneities and decreasing the density of deep traps is necessary, as well as extending the measurements to heterojunctions with lower electron concentration in the buffer, and ternary films with various Al compositions.

ACKNOWLEDGMENTS

REFERENCES

[1]S. I. Stepanov, V. I. Nikolaev, V. E. Bougrov, and A. E. Romanov, Rev. Adv. Mater. Sci. **44**, 63–86 (2016), see http://www.ipme.ru/e-journals/RAMS/no_14416/06_14416_stepanov.pdf.

[2]S. J. Pearton, J. Yang, P. H. Cary, F. Ren, J. Kim, M. J. Tadjer, and M. A. Mastro, Appl. Phys. Rev. **5**, 011301 (2018).

[3]Z. Galazka, Semicond. Sci. Technol. **33**, 113001 (2018).

[4]M. A. Mastro, A. Kuramata, J. Calkins, J. Kim, F. Ren, and S. J. Pearton, ECS J. Solid State Sci. Technol. **6**, P356 (2017).

[5]S. J. Pearton, F. Ren, M. Tadjer, and J. Kim, J. Appl. Phys. **124**, 220901 (2018).

[6]J. Li, X. Chen, T. Ma, X. Cui, F.-F. Ren, S. Gu, R. Zhang, Y. Zheng, S. P. Ringer, L. Fu, H. H. Tan, C. Jagadish, and J. Ye, Appl. Phys. Lett. **113**, 041901 (2018).

[7]R. Wakabayashi, M. Hattori, K. Yoshimatsu, K. Horiba, H. Kumigashira, and A. Ohtomo, Appl. Phys. Lett. **112**, 232103 (2018).

[8]E. Ahmadi, O. S. Koksaldi, X. Zheng, T. Mates, Y. Oshima, U. K. Mishra, and J. S. Speck, Appl. Phys. Express **10**, 071101 (2017).

[9]Y. Zhang, C. Joishi, Z. Xia, M. Brenner, S. Lodha, and S. Rajan, Appl. Phys. Lett. **112**, 233503 (2018).

[10]Y. Zhang, A. Neal, Z. Xia, C. Joishi, J. M. Johnson, Y. Zheng, S. Bajaj, M. Brenner, D. Dorsey, K. Chabak, G. Jessen, J. Hwang, S. Mou, J. P. Heremans, and S. Rajan, Appl. Phys. Lett. **112**, 173502 (2018).

[11]S. Krishnamoorthy, Z. Xia, C. Joishi, Y. Zhang, J. McGlone, J. Johnson, M. Brenner, A. R. Arehart, J. Hwang, S. Lodha, and S. Rajan, Appl. Phys. Lett. **111**, 023502 (2017).

[12]Y. Zhang, Z. Xia, J. McGlone, W. Sun, C. Joishi, A. R. Arehart, S. A. Ringel, and S. Rajan, IEEE Trans. Electron Devices **66**, 1574 (2019).

[13]T. Oshima, Y. Kato, N. Kawano, A. Kuramata, S. Yamakoshi, S. Fujita, T. Oishi, and M. Kasu, Appl. Phys. Express **10**, 035701 (2017).

[14]A. Y. Polyakov, N. B. Smirnov, I. V. Shchemerov, S. J. Pearton, F. Ren, A. V. Chernykh, and A. I. Kochkova, Appl. Phys. Lett. **113**, 142102 (2018).

[15]A. Y. Polyakov, N. B. Smirnov, I. V. Shchemerov, D. Gogova, S. A. Tarelkin, and S. J. Pearton, J. Appl. Phys. **123**, 115702 (2018).

[16]A. Y. Polyakov, N. B. Smirnov, I.-H. Lee, and S. J. Pearton, J. Vac. Sci. Technol. B **33**, 061203 (2015).

[17]E. B. Yakimov, A. Y. Polyakov, N. B. Smirnov, I. V. Shchemerov, J. Yang, F. Ren, G. Yang, J. Kim, and S. J. Pearton, J. Appl. Phys. **123**, 185704 (2018).

[18]A. Y. Polyakov, N. B. Smirnov, I. V. Shchemerov, E. B. Yakimov, J. Yang, F. Ren, G. Yang, J. Kim, A. Kuramata, and S. J. Pearton, Appl. Phys. Lett. **112**, 032107 (2018).

[19]A. Y. Polyakov, N. B. Smirnov, I. V. Shchemerov, S. J. Pearton, F. Ren, A. V. Chernykh, P. B. Lagov, and T. V. Kulevoy, APL Mater. **6**, 096102 (2018).

[20]L. Binet and D. Gourier, J. Phys. Chem. Solids **59**, 1241 (1998).

[21]A. Y. Polyakov, N. B. Smirnov, I. V. Shchemerov, E. B. Yakimov, S. J. Pearton, F. Ren, A. V. Chernykh, D. Gogova, and A. I. Kochkova, ECS J. Solid State Sci. Technol. **8**(7), Q3019 (2019).

[22]J. D. Lee, E. Flitsiyan, L. Chernyak, J. Yang, F. Ren, S. J. Pearton, B. Meyler, and Y. Joseph Salzman, Appl. Phys. Lett. **112**, 082104 (2018).

[23]Z. Zhang, E. Farzana, A. R. Arehart, and S. A. Ringel, Appl. Phys. Lett. **108**, 052105 (2016).

[24]K. Irmscher, Z. Galazka, M. Pietsch, R. Uecker, and R. Fornari, J. Appl. Phys. **110**, 063720 (2011).

[25]A. Y. Polyakov, N. B. Smirnov, A. V. Govorkov, E. A. Kozhukhova, S. J. Pearton, F. Ren, S. Y. Karpov, K. D. Shcherbachev, N. G. Kolin, and W. Lim, J. Vac. Sci. Technol. B **30**, 041209 (2012).

[26]C. Fares, F. Ren, D. C. Hays, B. P. Gila, M. Tadjer, K. D. Hobart, and S. J. Pearton, Appl. Phys. Lett. **113**, 182101 (2018).

[27]X. Z. Dang, C. D. Wang, E. T. Yu, K. S. Boutros, and J. M. Redwing, Appl. Phys. Lett. **72**, 2745 (1998).

[28]A. Y. Polyakov, N. B. Smirnov, I. V. Shchemerov, E. B. Yakimov, S. J. Pearton, C. Fares, J. Yang, F. Ren, J. Kim, P. B. Lagov, V. S. Stolbunov, and A. Kochkova, Appl. Phys. Lett. **113**, 092102 (2018).

[29]M. Meneghini, G. Meneghesso, and E. Zanoni, in *Trapping and Degradation Mechanisms in GaN-Based HEMTs*, in *Gallium Nitride (GaN) Physics, Devices, and Technology*, edited by F. Medjdoub and K. Iniewski (CRC Press, Boca Raton, 2013), Chap. 10.

[30]A. T. Neal, S. Mou, S. Rafique, H. Zhao, E. Ahmadi, J. S. Speck, K. T. Stevens, J. D. Blevins, D. B. Thomson, N. Moser, K. D. Chabak, and G. H. Jessen, Appl. Phys. Lett. **113**, 062101 (2018).

[31]D.-W. Jeon, H. Son, J. Hwang, A. Y. Polyakov, N. B. Smirnov, I. V. Shchemerov, A. V. Chernykh, A. I. Kochkova, S. J. Pearton, and I.-H. Lee, APL Mater. **6**, 121110 (2018).

[32]M. E. Ingebrigtsen, J. B. Varley, A. Y. Kuznetsov, B. G. Svensson, G. Alfieri, A. Mihaila, U. Badstübner, and L. Vines, Appl. Phys. Lett. **112**, 042104 (2018).

[33]J. F. McGlone, Z. Xia, Y. Zhang, C. Joishi, S. Lodha, S. Rajan, S. A. Ringel, and A. R. Arehart, IEEE Electron Dev. Lett. **39**, 1042 (2018).